

Monomeric and Tetrameric Forms of Petroporphyrin VO-EtioP-III: Effect of Solid-State Aggregation on Electronic Absorption Spectra

Yuriy A. Zhabanov,^{a,b} Alexey V. Eroshin,^a Oskar I. Koifman,^a Vladislav V. Travkin,^{a,b} and Georgiy L. Pakhomov^{a,b}

^aIvanovo State University of Chemistry and Technology, 153000 Ivanovo, Russian Federation

^bInstitute for Physics of Microstructures of the Russian Academy of Sciences, 603950 Nizhny Novgorod, Russian Federation

@Corresponding author E-mail: pakhomov@ipmras.ru

Recently, we have reported solid-state structure of vanadyl etioporphyrin-III (VO-EtioP-III) and its strong impact on the electronic absorption spectra [doi: 10.1002/slct.202303271]. VO-EtioP-III is one of the most abundant petroporphyrins, so issues related to its identification by optical methods in monomeric and aggregated forms require more detailed study. Here, the quantum chemical calculations of electronic structure of VO-EtioP-III as a single molecule and as a tetramer, geometry of which coincides with the unit cell, were used to assess the relationship between crystal packing and absorption spectra.

Keywords: Etioporphyrin molecule, DFT, aggregation, electronic absorption spectra.

Мономерная и тетрамерная форма петропорфирина VO-EtioP-III: влияние агрегации в твердой фазе на электронные спектры поглощения

Ю. А. Жабанов,^{a,b} А. В. Ерошин,^a О. И. Койфман,^a В. В. Травкин,^{a,b} Г. Л. Пахомов^{a,b}

^aФГБОУ ВО Ивановский государственный химико-технологический университет, 153000 Иваново, Российская Федерация

^bИнститут физики микроструктур Российской академии наук, 603950 Нижний Новгород, Российская Федерация

@E-mail: pakhomov@ipmras.ru

Недавно мы опубликовали данные о кристаллической структуре комплекса этиопорфирина-III с ванадилем, VO-EtioP-III, и ее влиянии на электронные спектры поглощения [doi: 10.1002/slct.202303271]. VO-EtioP-III – один из наиболее распространенных петропорфиринов, поэтому вопросы, касающиеся его идентификации оптическими методами в мономерном или агрегированном состоянии, заслуживают более пристального изучения. В данной работе, для оценки влияния кристаллической упаковки на спектры поглощения были использованы квантово-химические расчеты электронной структуры молекулы VO-EtioP-III и его тетрамера, соответствующего геометрии элементарной ячейки.

Ключевые слова: Этиопорфирин, DFT расчеты, агрегация, электронные спектры поглощения.

Introduction

Although petroporphyrins, including those of *etio*-type, are widespread in nature as components of solid fossil fuels,^[1] little is known about the properties of their molecules in the condensed state. In particular, the extent to which the aggregating molecules can mutually disturb their electronic clouds, and hence, modify the profile of the electronic absorption spectrum, has not been assessed. As shown recently,^[2] the experimental spectrum of VO-EtioP-III experiences an unexpectedly strong broadening of the Soret-band, accompanied by a shift of both Q- and Soret bands towards longer wavelengths, when going from diluted solution to crystalline film. Therefore, it is important to validate such a trend with theoretical arguments. In this work, electronic absorption spectra of a free VO-EtioP-III molecule and the unit cell structure in a crystal (with $Z=4$, *i.e.* tetramer^[2]) were numerically simulated, interpreted and directly compared with the experimental results.

Methodology

Experimental details related to the synthesis and characterization of VO-EtioP-III in solutions, crystals, and thin films have been published elsewhere.^[2] The preliminary optimization of geometry of the VO-EtioP-III molecule was carried out using density functional theory, DFT (PBEh-3c functional^[3]). The experimentally determined geometry of the unit cell^[2] was taken as the tetramer structure and not optimized due to the complexity of this procedure. Since the monomeric form of VO-EtioP-III is an open-shell compound, spectral bands were simulated on the base of the simplified time-dependent density functional theory (sTD-DFT) approach^[4,5] implemented in an ORCA 5.0.3 software.^[6,7] To visualize the theoretical spectrum, each peak was modeled using Lorentz functions, with the oscillator strength equal to the peak area. The half-width of the peaks (30 nm) was adjusted to achieve the best match between the graphical image of the simulated spectrum and the experimental one.

We were interested here in analyzing the behavior of basic absorption bands in a solid rather than in reproducing experimental spectra, therefore a single unit cell of VO-EtioP-III was taken as a model. This is, of course, a very rough approximation because such an arrangement is continuously translated in all directions of a crystal lattice and molecules in neighboring unit cells interact as well. However, as shown below, it can adequately describe the trend observed in experiment. Tetramer model was also used for TD-DFT calculations in Ref.^[8] to distinguish between optical spectra of monoclinic and triclinic crystal phases of lead phthalocyanine, a kindred non-planar porphyrin compound. Analysis of the electron density distribution was performed by the quantum theory of atoms in molecules (QTAIM) method using an AIMALL program.^[9]

Results and Discussion

In the calculated spectrum of monomeric VO-EtioP-III, the weak Q-band consists predominantly of transitions from the highest occupied molecular orbital to the lowest unoccupied molecular orbital, HOMO→LUMO. Molecular orbitals (MO) level diagram for VO-EtioP-III is presented in Figure 1. It is worth comparing obtained results with previously studied extraligated complex of *etio*-porphyrin-I with indium(III), InCl-EtioP-I.^[10] Although the calculation was carried out for asymmetric VO-EtioP-III molecule (C_1

full point group, true symmetry of all orbitals is 'a'), for a better comparison we marked the symmetry of orbitals to correspond to C_4 point group (Figure 1 and Table S1). The HOMO-LUMO gap of VO-EtioP-III (ΔE in Figure 1) was found to be greater by *ca.* 0.7 eV than that of InCl-EtioP-I due to the differences in symmetry and shrinkage of the coordination cavity. The latter circumstance is likely associated with a smaller ionic radius of vanadium^[11] and, possibly, a different nature of axial ligand (oxygen instead of chlorine in InCl-EtioP-I). This amends the ligand geometry and, consequently, shifts the energies of both HOMO and LUMO located on the macrocyclic core. The increase in the calculated ΔE value correlates with the blue shift of Q-band observed in a dilute solution of VO-EtioP-III in chloroform relative to a similar solution of InCl-EtioP-I (Figure S1).

The most intensive band is located at 381 nm in the Soret region and consists of the electronic transitions from HOMO-1 and HOMO to doubly-degenerated LUMO (Figure 1, Table S1). The shapes of the frontier orbitals are typical of many other porphyrins and their analogues.^[10,12-15]

As can be seen from Figure 2, the experimental and calculated spectra of isolated VO-EtioP-III molecule qualitatively coincide. In the calculated spectrum of the tetramer, the absorption bands are composed by many electronic transitions; the largest contribution of any of them does not exceed 10% (Figure 3). These new bands in the tetramer spectrum are often not resolved experimentally, but manifest themselves as the "broadening" of observed peaks. The deconvolution of experimental spectrum of VO-EtioP-III film gives at least 4 Gaussian components of the Soret-band, with the main peak being redshifted by ~7 nm relative to the spectrum in chloroform (Figure S2). The main electronic transitions in monomeric and tetrameric forms of VO-EtioP-III obtained by DFT are collected in Tables S1 and S2 respectively, along with corresponding oscillator strengths. The blue shift of the simulated spectrum occurs through the use of the vertical transition approximation. Vertical excitation energies in such calculation procedures are usually slightly overestimated.^[14]

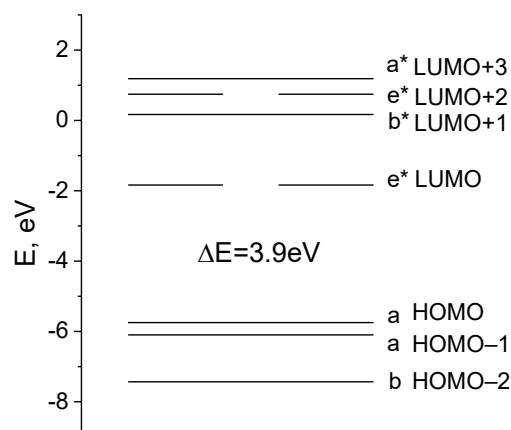


Figure 1. Molecular orbitals (MO) level diagram for VO-EtioP-III. Indicated orbitals symmetry corresponds to the molecule of C_4 symmetry, which was used earlier for DFT study of InCl-EtioP-I molecule,^[10] see text. Vacant orbitals are marked with an asterisk.

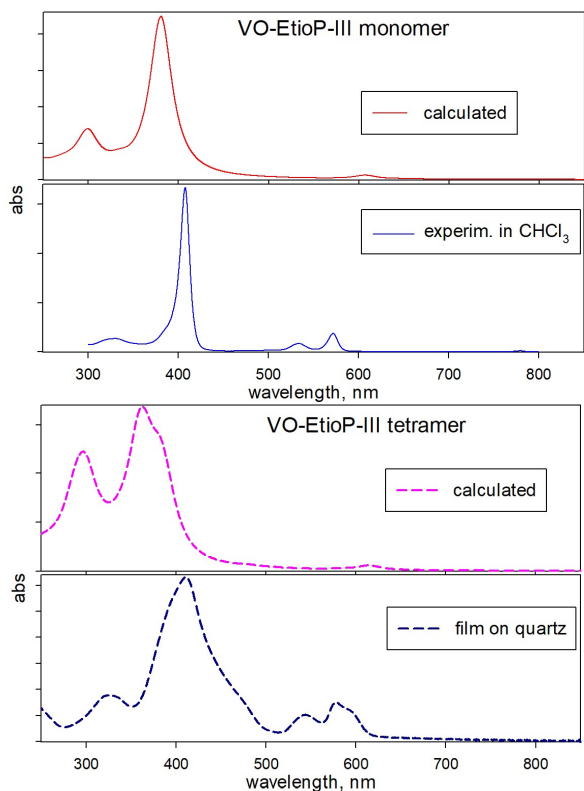


Figure 2. Comparison of the calculated spectrum of monomer with spectrum of VO-EtioP-III in chloroform solution (left panels) and calculated spectrum of tetramer with spectrum of a 70 nm thick vacuum-deposited film on quartz substrate (right panels).

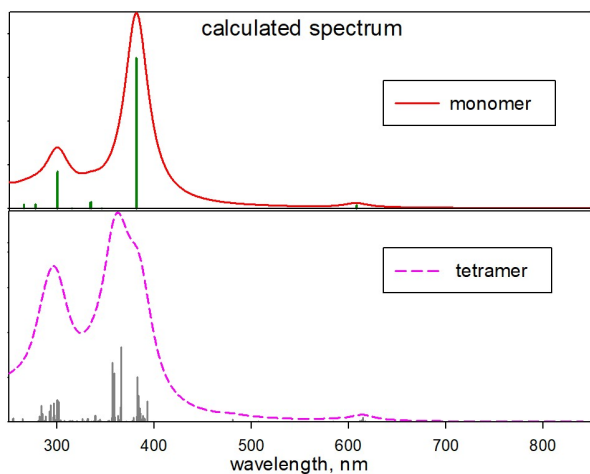


Figure 3. The calculated electronic absorption spectra of monomeric and tetrameric forms of VO-EtioP-III.

Both the experimentally detected shift and the broadening of the Soret-band in a film fit perfectly with those in the simulated spectrum of a tetramer (Figure 2). Now we can distinguish between these two effects: the first is a bathochromic shift of the main maximum by 16 nm, the second is appearance of new bands in the long wavelength range of 380–390 nm due to splitting (not just solid-state broadening of “monomeric” bands) (Figures 3 and S2). Therefore, the observed spectral changes are fully con-

sistent with the electronic processes theoretically expected for VO-EtioP-III molecules aggregated in a manner that conforms to the crystal structure. In addition, we gain an indirect argument that the unit cell structure persists in the thin vacuum-deposited film, which could not be reliably detected by X-ray diffraction.^[2]

Considering the DFT results for a tetramer, following points should be highlighted:

1) Slight distortion of the shape of HOMO and LUMO orbitals in the aggregated molecules is responsible for the redshift of the absorption edge of films compared to the monomer spectrum.

2) MOs can be localized on either one or two molecules (Table S2). The π -stacked molecules in the unit cell (seen as “dimer” in the centre of Figure 4) have common molecular orbitals. However, despite the general similarity of the calculated shapes of orbitals in monomeric and tetrameric structures, differences due to aggregation were found out. For instance, the electron density is shifted by one half of the molecule in the case of the α -HOMO-16 molecular orbital involved in the electronic transitions that contribute to a medium-intensive band at 383 nm (oscillator strength is 0.35) in the Soret region, as illustrated in Figure 5. Thereby, new bands associated with intramolecular charge transfer emerge. Other orbitals involved in the electronic transitions are distorted less noticeably.

3) While only one band was observed for monomer [381(1.03)], distortion of orbitals by intermolecular interaction results in four intense peaks [392(0.27), 383(0.35), 382(0.6), 366 (1.0) and 359(0.65)] in the tetramer spectrum (*cf.* Figure S2). As mentioned above, this explains why splitting and redshift of the experimental Soret-band occur. The band with $\lambda_{\max} = 392$ nm deserves special attention. Its presence in the tetramer simulated spectrum suggests intermolecular electronic transitions from the central (π -stacked, dimeric) molecules in the unit cell to the orthogonally positioned ones (Table S2).

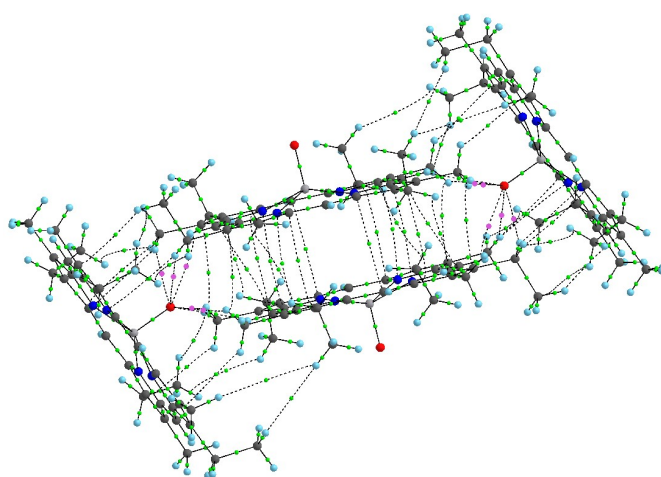


Figure 4. Bond critical points (BCPs) according to the analysis of the electron density distribution by QTAIM method. BCPs between oxygen of orthogonally positioned molecules (on the left and on the right) and ethyl and methyl groups of the central molecules are marked by pink balls.

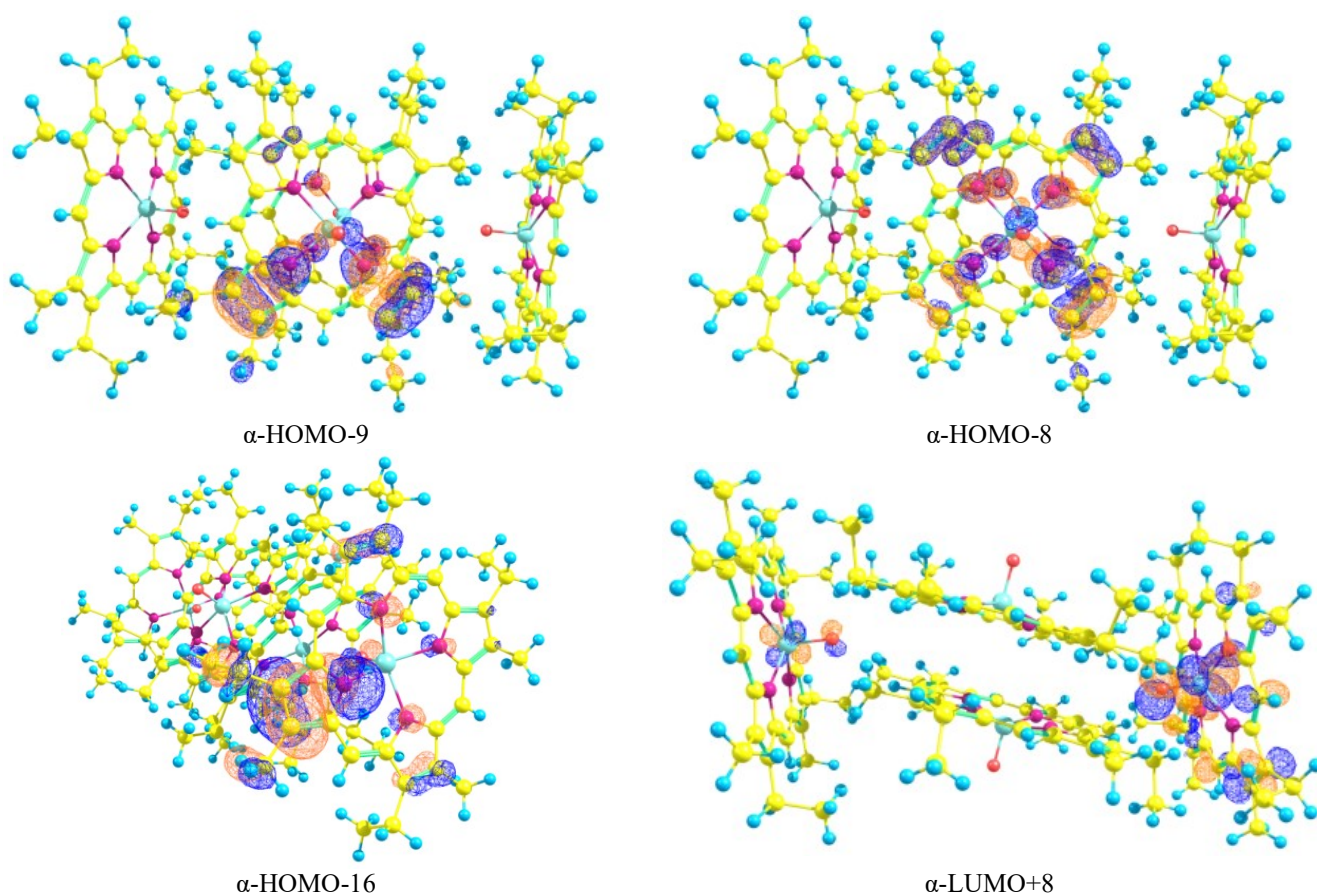


Figure 5. Examples of distorted molecular orbitals in the unit cell of VO-EtioP-III.

4) Splitting of the less intense absorption band at *ca.* 300 nm predictably occurs in the tetramer spectrum, too (Figure 3). In case of a monomer, this peak predominantly corresponds to the electronic transitions from HOMO-5, localized on the nitrogen and C $_{\beta}$ atoms, to LUMO (Table S1). The tetramer spectrum contains 9 peaks with approximately equal intensity ($f=0.24\pm 0.08$). Four of them correspond to electronic transitions between orbitals of similar shape but localized on different molecules composing the unit cell. In other words, for each tetramer molecule we do see the same transitions from HOMO-5 to LUMO as in the monomer, with one peak splitting into four without changing the position of the overall maximum. However, there exist five ligand-to-metal charge transfer (LMCT) transitions that can be considered as analogous to electronic transitions from HOMO and HOMO-1 to LUMO+2 in monomer, responsible for bands at 277 and 265 nm in its spectrum. Note, that LUMO+2 predominantly contains AOs of vanadium and oxygen. Intermolecular interaction should affect the energy of such type orbitals belonging to the orthogonal molecules in the unit cell, thus causing slight bathochromic shift. Therefore, the spectrum of the tetramer shows a more complex absorption peak at *ca.* 300 nm than the monomer consisting of a number of subpeaks. Yet, their relative intensities and energy positions prevent the resulting peak from being visually displaced (Figure 3).

5) According to the QTAIM calculations, there are a number of bond critical points (BCP) between molecules in

the tetramer, as shown in Figure 4. This indicates multiple intermolecular interactions.^[16] The most important feature are BCPs between axial ligand (oxygen) of the orthogonally positioned molecules and ethyl or methyl groups of the molecules forming the “dimer” in the centre, marked in pink in Figure 4 (see, comment #4 above). Three of these points correspond to the shortest distances between axial oxygen of the orthogonally positioned molecules and the hydrogen atoms in the central molecules in the unit cell,^[2] implying hydrogen bonding.

It should be noted that the experimentally measured electronic absorption spectra of VO-EtioP-III films remarkably depend on their thickness (Figure S2). This is not surprising, since morphology of vacuum-deposited molecular layers may vary with thickness,^[8] the reason being the different size and orientation of the ordered domains (molecular stacks or crystallites) relative to the substrate surface. Thus, spectral changes reflect different form-factor (habit) of the crystallites forming the VO-EtioP-III film,^[2] which determines the actual aggregation length, *i.e.* the maximum units involved in intermolecular interaction in the selected projection. Unfortunately, theoretical approach used does not allow the modeling systems with an infinitely expanded molecular composition. It is also possible to deliberately select tetramers with a different molecular arrangement within the same crystal lattice and model their spectra theoretically, the work is underway.

Conclusion

The relevancy of experimentally observed changes in the optical spectra of VO-EtioP-III molecules upon transition from monomeric to aggregated (crystals or films) form is theoretically proven. The reason underlying bathochromic shift of two bands in the visible range and strong broadening of the Soret-band is the distortion of several MOs by intermolecular interactions that also comprise hydrogen bonding. Analysis of quantum chemical calculation data shows that consideration of a one elected unit cell is sufficient to qualitatively explain the effect of aggregation on the electronic structure of the VO-EtioP-III molecule.

Acknowledgements. This work was supported by RSF Grant #20-13-0028. The authors are grateful to Prof. J.-M. Ribo (UB) for expert guidance and advices.

References

1. Gray M., Yarranton H., Chacón-Patiño M., Rodgers R., Bouyssière B., Giusti P. *Energy Fuels* **2021**, *35*, 18078–18103; doi: 10.1021/acs.energyfuels.1c01837.
2. Pakhomov G.L., Koptyaev A.I., Yunin P.A., Somov N.V., Semeikin A.S., Rychikhina E.D., Stuzhin P.A. *Chemistry Select* **2023**, *8*, e202303271; doi: 10.1002/slct.202303271.
3. Grimme S., Brandenburg J.G., Bannwarth Ch., Hansen A. *J. Chem. Phys.* **2015**, *143*, 054107; doi: 10.1063/1.4927476.
4. Bannwarth Ch., Grimme S. *Comput. Theor. Chem.* **2014**, *1040–1041*, 45–53; doi: 10.1016/j.comptc.2014.02.023.
5. Martynov A.G., Mack J., May A.K., Nyokong T., Gorbunova Y.G., Tsivadze A.Yu. *ACS Omega* **2019**, *4*, 7265–7284; doi: 10.1021/acsomega.8b03500.
6. Neese F. *WIREs Comput. Mol. Sci.* **2012**, *2*, 73–78; doi: 10.1002/wcms.81.
7. Neese F. *WIREs Comput. Mol. Sci.* **2022**, *12*, e1606; doi: 10.1002/wcms.1606.
8. Kato M., Yoshizawa H., Nakaya M., Kitagawa Y., Okamoto K., Yamada T., Yoshino M., Tanaka K., Onoe J. *Sci. Rep.* **2022**, *12*, 8810; doi: 10.1038/s41598-022-12990-z.
9. Keith T.A. *TK AIMAll Version 16.01.09*. Gristmill Software, Overland Park KS, USA, **2017**. <https://aim.tkgristmill.com>.
10. Koifman O.I., Rychikhina E.D., Travkin V.V., Sachkov Y.I., Stuzhin P.A., Somov N.V., Yunin P.A., Zhabanov Y.A., Pakhomov G.L. *ChemPlusChem* **2023**, *88*, e202300141; doi: 10.1002/cplu.202300141.
11. Shannon R.D. *Acta Crystallogr., Sect. A* **1976**, *32*, 751–767; doi: 10.1107/S0567739476001551.
12. Eroshin A.V., Otyotov A.A., Kuzmin I.A., Stuzhin P.A., Zhabanov Y.A. *Int. J. Mol. Sci.* **2022**, *23*, 939; doi: 10.3390/ijms23020939.
13. Belosludov R.V., Nevenon D., Rhoda H.M., Sabin J.R., Nemykin V.N. *J. Phys. Chem. A* **2019**, *123*, 132–152; doi: 10.1021/acs.jpca.8b07647.
14. Nemykin V.N., Hadt R.G., Belosludov R.V., Mizuseki H., Kawazoe Y. *J. Phys. Chem. A* **2007**, *111*, 12901–12913; doi: 10.1021/jp0759731.
15. Travkin V.V., Semikov D.A., Stuzhin P.A., Skvortsov I.A., Pakhomov G.L. *Appl. Sci.* **2023**, *13*, 1211; doi: 10.3390/app13021211.
16. Bader R.F.W. *Atoms in Molecules. In: Encyclopedia of Computational Chemistry, John Wiley & Sons, Ltd: Chichester, UK, 2002*; doi: 10.1002/0470845015.caa012.

Received 16.01.2024

Accepted 21.02.2024